PFC/JA-94-20

Papers Presented at the 21st EPS Conference on Controlled Fusion and Plasma Physics by the Alcator C-Mod Group (Montpellier, France, June 27 - July 1, 1994)

Plasma Fusion Center
Massachusetts Institute of Technology
Cambridge, MA 02139

July 1994

This work was supported by the U. S. Department of Energy Contract No. DE-AC02-78ET51013.

Papers Presented at the 21st EPS Conference
on Controlled Fusion and Plasma Physics by the Alcator C–Mod Group

Table of Contents

[†]ENEA, Frascati.
[‡]University of Maryland.
[*]Johns Hopkins University

Institute of Physics Publishing **0** (1993) 1–6. Printed in the UK

Confinement and divertor studies in Alcator C-Mod

I H Hutchinson, R Boivin, F Bombarda†, P Bonoli, C Fiore, J Goetz, S Golovato, R Granetz, M Greenwald, S Horne, A Hubbard, J Irby, B LaBombard, B Lipschultz, E Marmar, G McCracken, M Porkolab, J Rice, J Snipes, Y Takase, J Terry, S Wolfe, B Welch‡, C Christensen, D Garnier, M Graf, T Hsu, D Jablonski, C Kurz, T Luke, M May§, A Niemczewski, P O'Shea, J Schachter, P Stek, G Tinios

Plasma Fusion Center, Massachusetts Institute of Technology, Cambridge, MA, 02139, USA.

Abstract. Early results from the Alcator C-Mod tokamak indicate that ohmic energy confinement does not obey the Neo-Alcator scaling. Instead 'Ohmic L-mode' confinement, close to ITER89-P, is obtained, which substantially exceeds Neo-Alcator under some circumstances. ICRF-heated plasmas follow the same scaling. H-modes are observed both in ohmic and ICRF heated plasmas, with confinement enhancements of about 2 for ELM-free conditions. Divertor operation into the closed chamber shows different regimes, depending on the density. Of particular interest is the progressive pressure detachment at moderate to high densities. Power to the divertor plates is generally low, reflecting the influence of strong radiation in the divertor. The scaling of parameters from Alcator's growing edge database is briefly summarized.

1. Introduction

The Alcator C-Mod tokamak (R=0.67m, a=0.21m) has operated so far at toroidal fields up to 5.3T and plasma currents up to 1 MA [1]. This paper gives an overview of early results in the areas of confinement and divertor studies.

Plasma densities up to 3×10^{20} m^{-3} have been obtained with gas puffing, limited primarily by marfe onset followed by radiative plasma boundary detachment and subsequent disruption. This occurs well below the Greenwald density limit even though the plasma purity appears good; $Z_{\rm eff} \sim 1$. Fuelling up to the Greenwald limit (highest value 10^{21}m^{-3}) has been achieved with deuterium pellet injection.

The flexible shaping of the tokamak has been used to produce plasmas with elongations of $1 \lesssim \kappa \lesssim 1.7$. Limiter operation uses the inboard cylinder as a limiter while diverted operation has used primarily the shaped closed divertor plates installed at the bottom of the machine. All plasma-facing components are molybdenum, although there are substantial areas of stainless-steel vacuum chamber far from the

† ENEA Frascati

‡ University of Maryland

§ Johns Hopkins University

/93/010001+06$07.50

plasma that are uncovered. Conditioning of the surfaces is primarily by electron cyclotron discharge-cleaning in hydrogen or deuterium using ≤ 3 kW at 2.45 GHz.

2. Confinement

The bulk of the confinement data obtained so far has been using ohmic heating alone. Nevertheless experiments with strong ICRF heating have recently begun, as discussed in Section 2.1. Section 2.2 discusses the observed scaling trends. H-mode observations are summarized in section 2.3.

2.1. ICRF Heating

Initial ICRF coupling studies were performed in 1993 using a radially movable monopole antenna. Up to 1.0 MW of RF power was injected at a power density up to 10 MW/m^2 and initial indications of both electron and ion heating were observed. The plasma loading was typically 5–20 Ω (10–40 times the vacuum loading), in qualitative agreement with predictions of full-wave calculations [2].

Two dipole antennas are now installed, and up to 4 MW of source power at 80 MHz will soon be available. The operating mode is hydrogen minority heating in deuterium majority plasmas at 5.3 T. In the future, ^{3}He minority heating will be used in deuterium majority plasmas at 7.9 T.

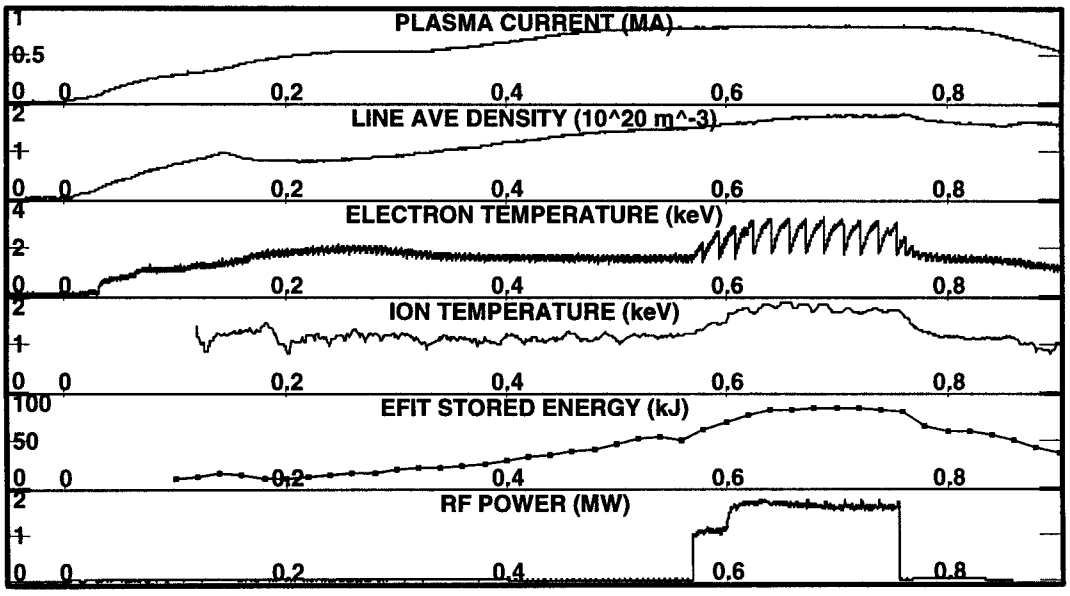

Figure 1. An ICRF-heated plasma.

Up to 1.8 MW of RF power has so far been coupled into the plasma from one dipole antenna [3]. Extensive conditioning of the TiC-coated antenna was *not* required to achieve this power level. Production of molybdenum impurities is observed to be reduced by a factor of five or more compared to operation with the monopole antenna.

A typical ICRF heated discharge is shown in Fig. 1. The target plasma was an inner-wall limited plasma of elongation 1.5 at a density of $\bar{n}_e = 1.8\times10^{20}\,\mathrm{m}^{-3}$ with a hydrogen minority concentration of approximately 10%. With the injection of 1.65 MW of RF power the stored energy as determined by EFIT magnetic equilibrium reconstruction increases from 52 to 85 kJ. The sawtooth amplitude and period increase markedly, as is often the case with ICRF heating, and the electron temperature (at the top of sawteeth) as determined from electron cyclotron emission approximately doubles to 3.2 keV. The ion temperature also increases strongly. Meanwhile, the ohmic heating power drops from 1.1 to 0.8 MW. From the discontinuity in slope of the diamagnetic stored energy at RF turn-on and turn-off, the absorption efficiency is estimated to be very high (80–100%). This is consistent with the observed energy increases under conditions of L-mode confinement, as discussed below.

2.2. Confinement performance and Scaling

High field, high power-density experiments are particularly interesting from the viewpoint of confinement scaling because they explore directions in parameter-space that tend to have little variation in the data of other experiments (see for example [4]). One aspect of this unique role is that for a high-field compact machine such as Alcator, L-mode (and H-mode) confinement can be substantially higher than that computed with neo-Alcator scaling – even under conditions of strong auxiliary heating. If confinement followed neo-Alcator, it would have the effect of limiting the performance of this class of machines. More fundamentally, broadening the data base may help us to understand the underlying causes of the variation of confinement time with density in linear ohmic, saturated ohmic, and auxiliary heated conditions.

Confinement data presented here uses the kinetic diagnostics of the plasma parameters to determine the stored energy. Electron temperature profiles are measured by electron cyclotron emission, density profiles from the 10-chord CO_2 interferometer, ion temperatures from neutron rates and high-resolution x-ray spectroscopy of argon lines and Z_{eff} from visible bremsstrahlung. The total heating input power is used (no corrections being made for radiation or RF absorption efficiency) and steady conditions are chosen so that energy time-derivatives are very small.

A striking difference has been observed in the ohmic confinement behaviour of Alcator C-Mod compared with its predecessor, Alcator C, whose results led to the Neo-Alcator scaling, $\tau_E = 0.192 \times 10^{-20}\bar{n}_e R^{2.04} a^{1.04} \kappa^{1/2}$ s. Even though the major radius of Alcator C-Mod is essentially the same as Alcator C, so that the machines are similar in many respects, we observe only very weak density-dependence of the energy confinement in C-Mod. Instead, we see a substantial plasma current dependence that was not present in the earlier machine's data.

This is illustrated in figure 2, where we show the confinement time plotted against density. Different groupings of plasma current are indicated by different symbols. There is little or no systematic scaling of τ_E with $\bar{n}$. The Neo-Alcator scaling

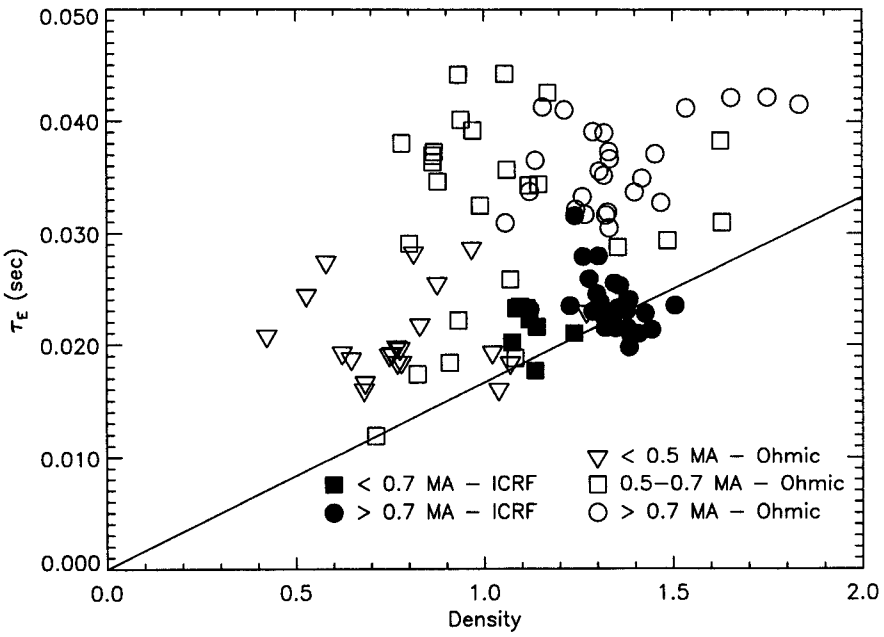

Figure 2. Energy confinement versus density. The line indicates the Neo-Alcator Scaling.

(appropriate for the bulk of the data – taking $\kappa = 1.5$, $R = .67$, and $a = .21$) is indicated. At the lower densities, the observed confinement exceeds that scaling by a factor of two or more.

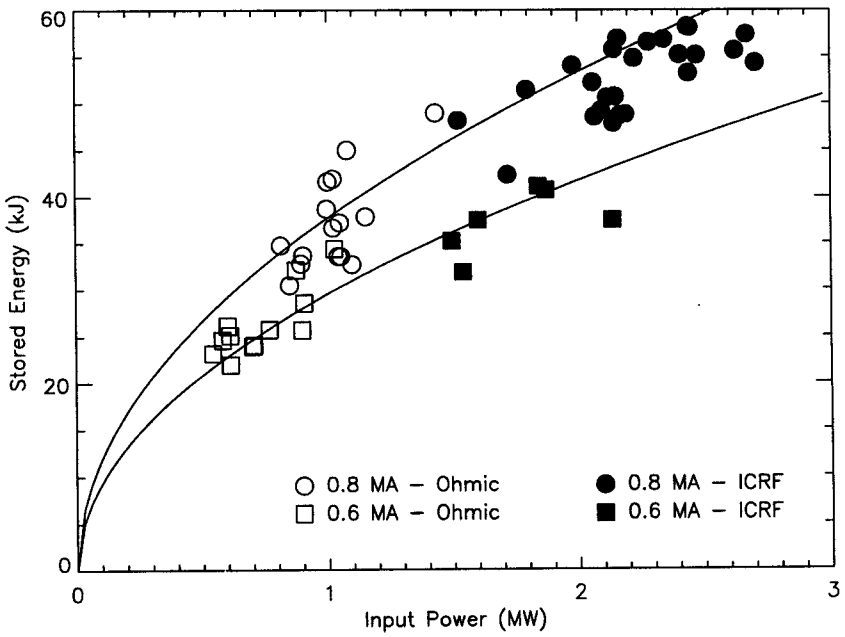

Figure 3. Power-scaling of the energy confinement time. Two data sets with currents 0.55—0.65 MA and 0.75–0.85 MA are shown. The lines indicate their ITER89-P scaling values.

Figure 3, by contrast, shows that the confinement agrees very well with the ITER89-P scaling

$$\tau_E = 0.048(I_p/MA)^{0.85}R^{1.2}a^{0.3}\kappa^{0.5}(n_e/10^{20})^{0.1}B^{0.2}(m_i/m_p)^{0.5}(P/MW)^{-0.5}s.$$

The scaling fits both ohmic and the ICRF heated data. There are no obvious differences in the global scaling for these different heating regimes. For that reason, we refer to the ohmic transport as 'Ohmic L-mode'.

The reasons for this striking departure from previous ohmic scalings are not yet clear. The main differences between Alcator C-Mod and Alcator C are (1) Shaping: C was a circular machine. (2) Limiter configuration: C had poloidal localized limiters. (3) Vacuum chamber: close-fitting in C, very open in C-Mod. However identification of the dominant factor awaits systematic data at low elongation.

2.3. H-Mode

Alcator C-Mod plasmas enter the H-mode high confinement regime quite readily with ohmic heating alone [5]. More recently, ICRF heated H-mode discharges have also been obtained. No special wall conditioning techniques were required to achieve ELM-free H-modes. There is, however, some indication that the conditioning effects of lithium pellet injection into tokamak plasmas help to reduce the power threshold [6].

For ELM-free H-modes, the observed ratio of threshold surface-power-density P/S to $\bar{n}_e B_T$ is found to be slightly lower than the value 0.044 $(\mathrm{MW/m^2})/(10^{20}\ \mathrm{m^{-3}\ T})$, reported from ASDEX-Upgrade [7]. It is as much as a factor of two lower for ELMy H-modes (following lithium pellet injection). H-modes have been achieved with toroidal fields up to 5.35 T and line-average densities up to $1.8 \times 10^{20} m^{-3}$. ICRF power in the range of 1 to 1.5 MW has now increased the maximum observed threshold P/S to 0.33 MW $\mathrm{m^{-2}}$.

The observed enhancements in particle confinement during the H-mode are typically 50 to 100%. The energy confinement analysis is complicated by the rapidly changing density and stored energy and the short duration of the ELM-free H-modes, generally not much longer than the confinement time. Nonetheless, H-mode confinement enhancement factors of about 2 have been estimated.

Figure 4 shows an example of an ELMy H-mode into which a Li pellet was injected just after 0.8 sec. Here $B_T = 5.25$ T and $I_p = 0.86$ MA were both held constant during the H-mode. The characteristic drop in the H_α emission at about 0.74 sec indicates the transition to H-mode and the electron density starts to rise rapidly. The midplane H_α view indicates little cyclic ELM activity. However, ELMs with a repetition frequency of 5 to 6 kHz are clearly observed near the lower X point throughout the H-mode. Then, as the pellet enters the plasma, the density suddenly increases, as does the H_α emission from both the midplane and the divertor region. This density rise appears to quench the H-mode. However, during the period of about 40 msec after the pellet, while the density and H_α emission are decaying back to near their pre-pellet levels,

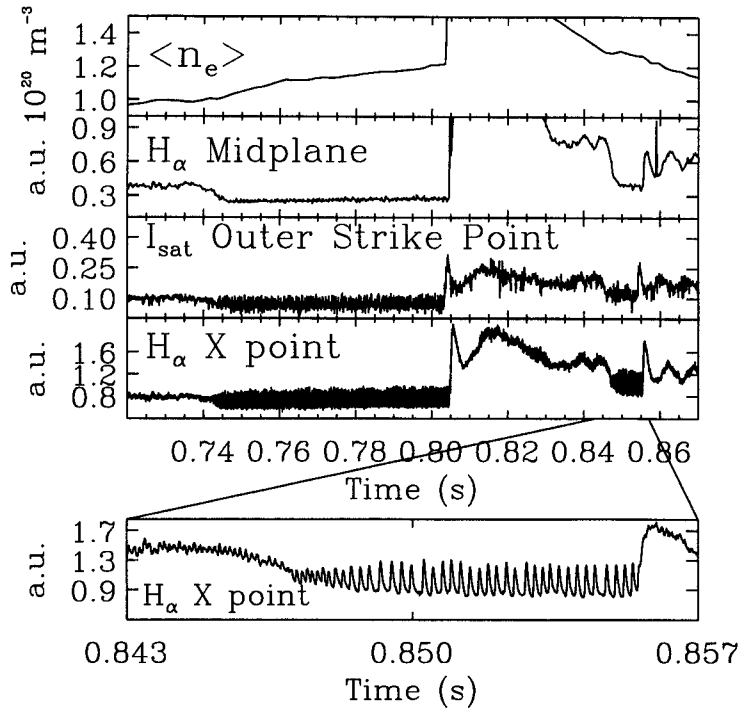

Figure 4. Lithium pellet injection into ohmic H-mode. The pellet is injected at 0.805s and causes the ELMy H-mode to revert to L-mode until about 0.846s when the H-mode reappears as the density decays away.

smaller amplitude and higher frequency (7.5 kHz) ELM-like oscillations persist. The end of this phase may be seen in the zoomed insert. Eventually, as the density from the pellet continues to decay, the midplane H_α emission once again suddenly drops into H-mode at about 0.846 sec and the ELMs gradually return to their pre-pellet amplitude and frequency.

3. Divertor

3.1. The closed divertor

Alcator C-Mod's closed, shaped divertor chamber is illustrated in figure 5. It is instrumented with probes embedded in the plates. Recently more of the flush probes have been replaced with domed probes so as to avoid ambiguous characteristics and provide complete density and temperature of profiles along the plate.

Figure 6 shows examples of these profiles mapped to the midplane flux-surface distance from the separatrix. The novel divertor geometry of Alcator C-Mod gives rise to 'inverted' temperature profiles that get hotter further from the separatrix up the 'vertical' plate. This is believed to be due to the enhanced ion source at the separatrix from neutrals recycling from the outer regions, which was the original motivation for this design. The effect has been documented recently in code studies [8]. Note in our data that the temperature begins to fall again along the upper face of the divertor, confirming the importance of geometry in determining the profiles.

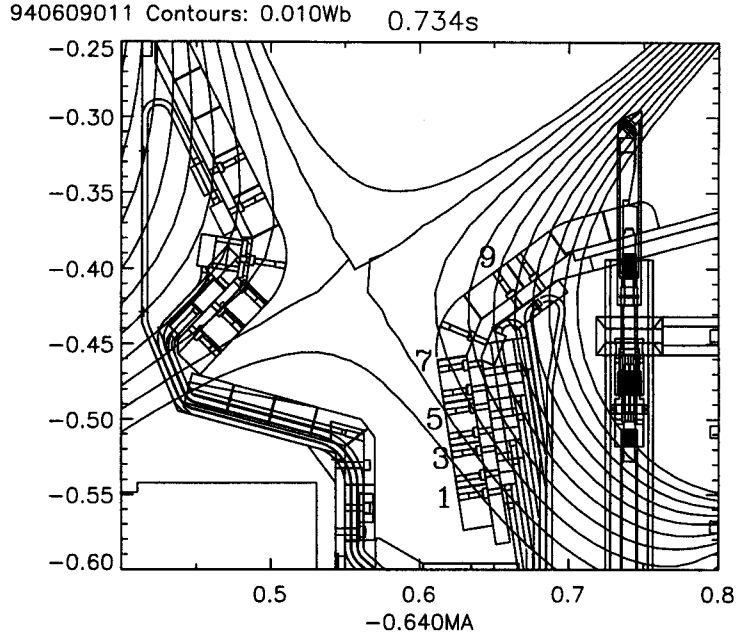

Figure 5. Layout of Alcator C-Mod's shaped divertor. The outer divertor embedded probes are numbered up the plate, and the reciprocating probe is also shown. The flux surfaces are those corresponding to the plasma of figure 6.

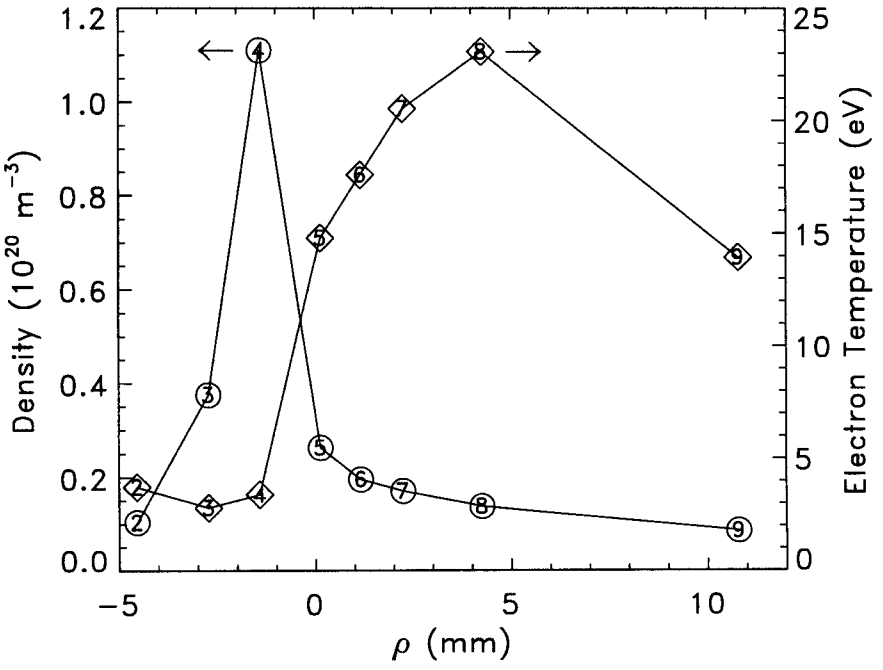

Figure 6. Outer divertor plate profiles. The data are mapped to midplane coordinate. Their position in the plate corresponds to the probe positions indicated in Fig. 5

A detailed description of the phenomena leading up to detachment of the plasma from the divertor plates has been given elsewhere [9]. In brief, the operation can be

divided into three regimes, as a function of $\bar{n}/I_p$. At low density, the plate temperature is close to the upstream temperature, and the SOL appears to be sheath-limited. As the density rises, the plate temperature drops and the plate density rises rapidly in a high-recycling mode of operation. In this regime, there is substantial divertor radiation loss, diagnosed with bolometers, up to 40% of the plasma input power. The divertor starts to detach locally, beginning in the private flux region, in this phase, and as the density rises the detachment progresses up the plate, preceded by a region of very high local plate density. The local detachment never passes above the 'nose' of the divertor. Instead, an abrupt global divertor detachment occurs, with precipitous drops in the plate density, while the temperature is at or below 5 eV. The density on the upper surface does not drop; it sometimes rises somewhat. The divertor radiation then moves upward and becomes dominant near the x-point.

3.2. Edge Scaling

The reciprocating Langmuir probe provides a complete profile of the edge density and electron temperature, which is invaluable for studying the scaling of edge parameters [10]. Data has been gathered over a wide density range and with plasma currents from 0.45 MA to 0.9 MA. The toroidal field was 5.3T throughout, so that both the safety factor (and hence field-line length) and also the total heating power (ohmic in this case) vary simultaneously with current. The spatial profiles are reasonably fitted by exponentials.

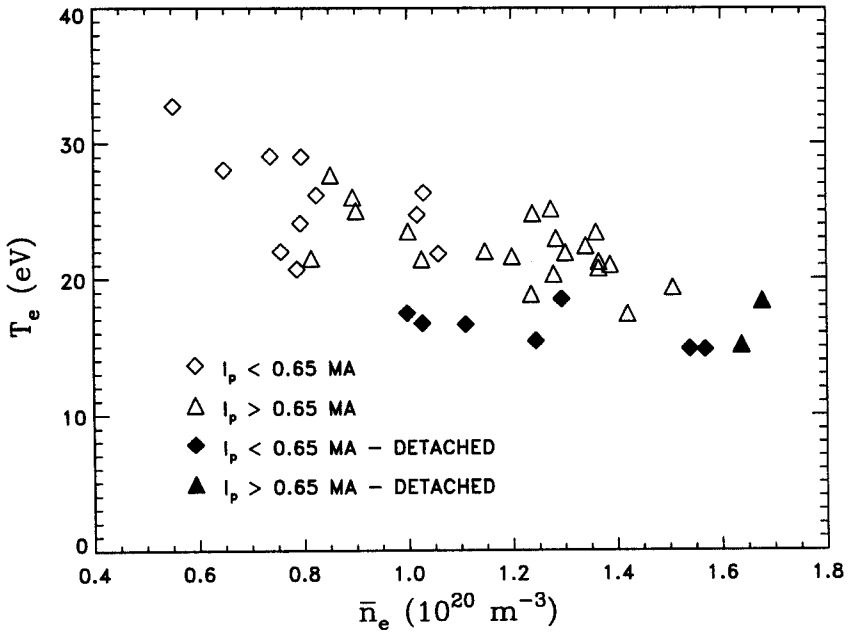

Figure 7. Edge temperature variation with main plasma line-average density. Triangles indicate currents between 0.65 and 0.9 MA; the diamonds range from 0.45 to 0.65 MA. Filled points are detached-divertor cases.

In figure 7 we plot the separatrix electron temperature as a function of line-average plasma density. In addition to the density dependence, it can be seen that there is

substantial current dependence, as indicated by the separation of higher and lower current points. There is no obvious discontinuity in the trends between the attached and detached divertor plasmas at this upstream location. There does seem to be a temperature threshold for detachment, but this might be more properly a reflection of a plate temperature threshold.

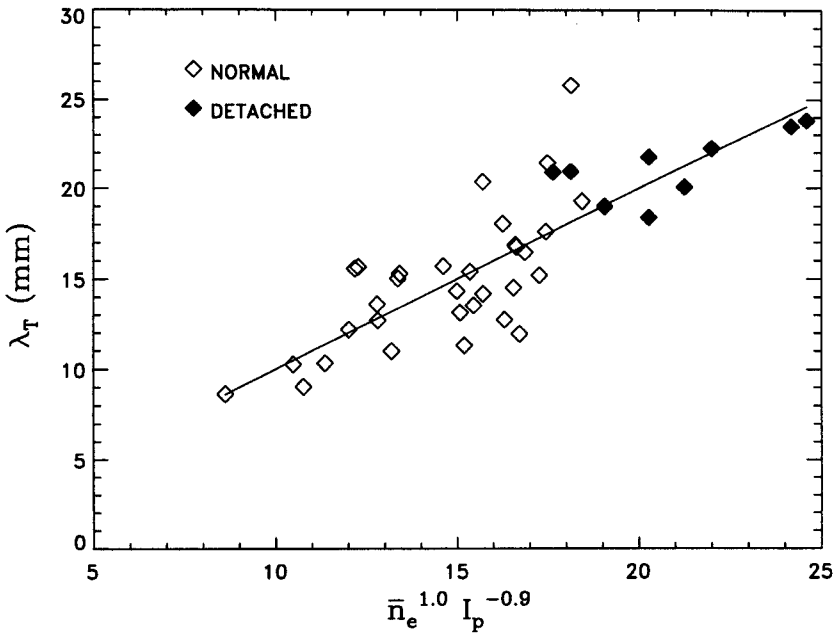

Figure 8. Edge temperature-width scaling regression against density and current.

In figure 8 we show a plot of a regression of the temperature-width versus the controlled parameters $\bar{n}_e$ and I_p. The regression scalings are $\lambda_T = 10\,(\bar{n}/10^{20}\mathrm{m}^{-3})^{1.0}(I_p/\mathrm{MA})^{-0.88}$ mm and $T_e = 29\,(\bar{n}/10^{20}\mathrm{m}^{-3})^{-0.73}(I_p/\mathrm{MA})^{0.69}$ eV. The standard error of the coefficients is about 0.1. These scalings may be compared with those observed in ASDEX [11] ($T_e \sim n^{-0.7}P^{0.5}$, power width $\sim q_a^{0.45}T_e^{-0.85}$) in the divertor, and JT-60 [12] (power width $\sim \bar{n}^{0.45}q_a^{0.67}P^{-0.49}$) at the plate.

The electron Spitzer conduction power down the SOL, estimated from the measured temperature and width, is only typically 10% of the ohmic power. This has been confirmed by computer simulations using the EDGE2D code, which show that the amount of power into the electrons cannot exceed about 0.1 MW if the reciprocating probe data is to be matched. Convection may carry perhaps somewhat more if a substantial fraction of the recycling is in the main chamber. However, it remains difficult to account for the power that is radiated in the vicinity of the x-point and below (so-called divertor radiation) [13], even for attached divertor cases, unless at least half of that power is supplied from field-lines inside the separatrix.

4. Conclusion

Alcator C-Mod's parameters are substantially different from those of the earlier

experiments whose data gave rise to the L-mode scaling, yet C-Mod's confinement is well described by the scaling. Our results also indicate that there is no significant difference between confinement in ohmic or auxiliary heated plasmas. These observations improve prospects for the unification of transport scaling and its understanding.

Divertor studies are revealing a wealth of complex phenomena. Some aspects of the divertor detachment are common to other experiments. However, the detailed diagnosis (just beginning) of the transition between the high-recycling regime and detachment is essential for understanding and controlling the power flow to the divertor plate.

Acknowledgments

The excellent engineering and technical support of the Alcator team is gratefully acknowledged. We are grateful to A.Loarte for running the EDGE2D code and valuable discussions. This work was supported by U.S. Department of Energy Contract No. DE-AC02-78ET5103.

References

[1] Hutchinson I H *et al* 1994 *Phys. Plasmas* **1** 1511
[2] Takase Y, Golvato S N, Porkolab M, Bonoli P T, Alcator Group 1994 *Fusion Engineering and Design* to be published
[3] Golovato S N *et al* 1994 *Controlled Fusion and Plasma Physics (Proc. 21th Eur. Conf. Montpellier)* (this conference)
[4] Christiansen J P, Cordey J G and Taroni A 1992 *Nucl. Fusion* **34** 375
[5] Snipes J, Granetz R S, Greenwald M, Hutchinson I H, Garnier D, Goetz J A, Golovato S, Hubbard A, Irby J, LaBombard B, Luke T, Marmar E S, Niemczewski A, Stek P C, Takase Y, Terry J L, Wolfe S M 1994 *Nucl. Fusion* to be published
[6] Snipes J, Granetz R S, Greenwald M, Hutchinson I H, Garnier D, Goetz J A, Golovato S, Hubbard A, Irby J, LaBombard B, Luke T, Marmar E S, Niemczewski A, Stek P C, Takase Y, Terry J L, Wolfe S M 1994 *Controlled Fusion and Plasma Physics (Proc. 20th Eur. Conf. Montpellier)* (this conference)
[7] Ryter F, Gruber O, Büchl K, Field A R, Fuchs C, Gehre, O, Herrmann A, Kaufmann M. Köppendörfer W, Mast F, Murmann H, Noterdaeme J-M, Pereverzev G V, Zohm H, ASDEX Upgrade and ICRH teams 1993 *Controlled Fusion and Plasma Physics (Proc. 20th Eur. Conf. Lisboa)* European Physical Society, Vol. 17C, Part I, I-23.
[8] Taroni A, Corrigan G, Radford G, Simonini R, Spence J, and Vlases G 1994 *Contrib. Plasma Phys.* **34** 448
[9] Lipschultz B, Goetz J, LaBombard B, McCracken G M, Terry J L, Graf M, Granetz R S, Jablonski D, Kurz C, Niemczewski A, and Snipes J 1994 *Proc. 11th International Conference on Plasma Surface Interactions, Mito, J. Nucl Mater.* to be published
[10] LaBombard B, Jablonski D, Lipschultz B, McCracken G, and Goetz J 1994 *Proc. 11th International Conference on Plasma Surface Interactions, Mito, J. Nucl Mater.* to be published
[11] McCormick K, Kyriakis G, Neuhauser J, Kakoulidis E, Schweinzer J, and Tsois N 1992 *J. Nucl. Mater.* **196-198** 264
[12] Itami K, Shimada M, and Hosogane N 1992 *J. Nucl. Mater.* **196-198** 755
[13] Goetz J A, Lipschultz B, Graf M A, Kurz C, Nachtrieb R, Snipes J A, and Terry J L 1994 *Proc. 11th International Conference on Plasma Surface Interactions, Mito, J. Nucl Mater.* to be published

ICRF EXPERIMENTS IN THE ALCATOR C-MOD TOKAMAK

S. N. Golovato, M. Porkolab, Y. Takase, R. Boivin,
P. Bonoli, F. Bombarda†, C. Fiore, J. Goetz, R. Granetz,
M. Greenwald, S. Horne, A. Hubbard, I. Hutchinson, J. Irby,
B. LaBombard, B. Lipschultz, E. Marmar, G. McCracken,
J. Rice, J. Snipes, J. Terry, S. Wolfe, B. Welch‡,
C. Christensen, D. Garnier, M. Graf, T. Hsu, D. Jablonski,
C. Kurz, T. Luke, M. May§, A. Mazurenko, A. Niemczewski,
P. O'Shea, J. Reardon, J. Schachter, P. Stek, G. Tinios

MIT Plasma Fusion Center, Cambridge, MA 02139, USA

Introduction Alcator C-Mod is a compact (R=0.67 m, a=0.21 m), high field (B $\lesssim$ 9 T), high current ($I_p < 3$ MA), shaped ($\kappa \leq 1.7$) tokamak. It has molybdenum plasma-facing components and can be run with a closed or open single-null divertor. The auxilliary heating required for studies of dissipative divertors and transport at high densities and magnetic fields is provided solely by ICRF. For the first phase of experiments, 2 MW of power at 80 MHz was available in up to 1 sec pulses and ICRF coupling studies were carried out using a radially movable single current strap antenna and accompanying radially movable outboard limiter. The goals of the first phase were to produce diverted plasmas appropriate for the second phase experiments with high power auxilliary heating and to establish the optimal outboard limiter and antenna positions for coupling high power to the diverted plasmas. The first phase experiments were carried out at 5.3 T and 1 MA plasma currents with up to 1 MW of ICRF power injected in the hydrogen minority heating regime in deuterium majority plasmas. A detailed description of Alcator C-Mod and the results of the first phase of experiments can be found elsewhere.[1]

For the second phase of experiments, 4 MW of power will be available and rf excitation will be achieved using two fixed position antennas, each with two toroidally spaced current straps which can be driven either in-phase or out-of-phase. The radial locations of the two-strap antennas and two fixed position outboard limiters were established in the first phase experiments. Initial results from the second phase of operation can be found elsewhere.[2] Presented here are the initial ICRF results on coupling and plasma heating with up to 1.8 MW of power injected using one two-strap antenna.

Single Current Strap Antenna Results In order to incorporate radial motion in the design of the first antenna, it was necessary that it retract into the 20 cm wide Alcator C-Mod port opening. To meet this constraint and still have an antenna spectrum that coupled effectively to the plasma, a single current strap design was required. The antenna had a two layer, titanium carbonitride (TiC/N) coated Faraday shield, TiC/N coated molybdenum protection tiles, and slotted side walls for better coupling to the plasma.[3] High plasma loading (5-20 Ω) was observed, which depended mainly on density and antenna-separatrix gap and high power operation was achieved (up to 1 MW, 13 MW/m^2) at relatively low rf voltages (<30 kV). At high power ($\gtrsim$200 kW) the loading was about 30% lower than that observed at low power ($\lesssim$ 10 kW). Heating powers in excess of 0.5 MW in pulse lengths up to 0.4 sec were applied to plasmas with peak densities of up to 4×10^{20} m^{-3} using gas fueling. Large increases in molybdenum radiation were observed at high rf power. The molybdenum radiation was reduced by about a factor of two when the density increased above 2×10^{20} m^{-3}. Increases in radiated power were estimated from bolometers to be as high as the applied rf power in some cases. Some plasma heating was observed with central electron temperature increases of up to 100 eV, as measured by electron cyclotron emission (ECE) and ion temperature increases of up to 500 eV, as measured by the fusion neutron rate. Analysis of charge exchange neutrals in low density discharges showed a high energy hydrogen distribution and deuterium bulk heating along with a high energy deuterium tail. The neutron rate measurement of ion heating may be an overestimate because of the non-thermal deuterium distribution. More details of the single-strap antenna results can be found elsewhere.[4]

---

† ENEA Frascati

‡ University of Maryland

§ Johns Hopkins University

The primary goal of these experiments was to study effects of the antenna and outboard limiter positions on coupling to diverted discharges. Using the radial motion capability of both the antenna and limiter, the following spacings were established for the fixed position limiters and two-strap antennas. The outboard limters are 2 cm from the separatrix, the antenna protection tiles are 5 mm behind the limiters, with the Faraday shield front face 5 mm behind the protection tiles. This geometry places the front face of the current straps 4.8 cm from the separatrix.

Two-Strap Antenna Results In order to have a good spectrum for ICRF coupling, the two-strap antennas had to be made significantly wider than a port opening. An additional benefit was to increase the surface area so that 2 MW of power could be coupled by one antenna at a power density of $\sim$ 10 MW/m^2. The disruption loads in Alcator C-Mod are very large, owing to the high field and plasma current capability, and the antennas and outboard limiters have to be fixed securely to the vacuum vessel wall to withstand these loads. This precluded the possibility of incorporating radial movement into the design. The first phase experiments played an important role by establishing the fixed radial locations of these antennas and limiters. The two-strap antennas have single-layer Faraday shields with side slots to faciliate rf flux coupling to the plasma. The two antennas have different Faraday shield coatings, one is TiC/N like the single-strap antenna, and the other Boron Carbide (B_4C). The antennas are located in adjacent ports such that they form a four element array with approximately equal strap spacing, allowing the possibility of future experiments using current drive phasing. There are B_4C-coated molybdenum protection tiles on the outside edges of the antennas but not between the antennas. This can be seen in Fig. 1, which shows the two two-strap antennas installed in Alcator C-Mod. More details on the design can be found elsewhere.[5]

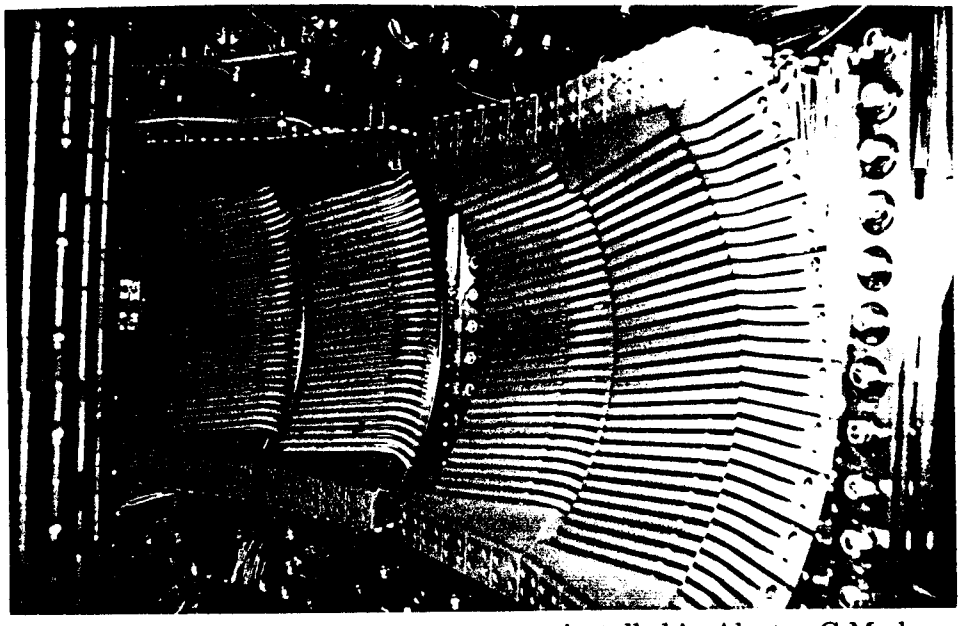

Figure 1 - The two two-strap antennas installed in Alcator C-Mod

The experiments described here have been carried out using only one of the two-strap antennas (TiC/N coated) with up to 2 MW of available rf power from a single transmitter. The second antenna will be operated shortly with an additional 2 MW of power from a second transmitter. Up to 1.8 MW has been coupled to the plasma using out-of-phase excitation of the two current straps (so-called dipole excitation), resulting in substantial plasma heating with significantly less impurity generation than was observed with the single-strap antenna. The heating follows L-mode scaling and brief periods of H-mode have been observed.[2]

Loading The plasma loading ranges from 3-25 Ohms depending on the density and antenna-separatrix spacing (outer gap), with the lowest loading observed during ELM-free H-mode periods. As with the single-strap antenna the loading is higher by about 25-30% at low power and decreases as the power is increased up to about 200 kW. Above 200 kW, the loading shows little power dependence. Figure 2 shows the loading resistance variation with line-averaged density for a set of limited discharges fueled by gas puffing. The different symbols correspond to data from

different days. The data shows a stronger than linear increase in loading with density. Using a Langmuir probe located in a protection tile of the single-strap antenna, it was observed that the density at the antenna rises faster than the central density as the gas fueling is increased. This information along with the data in Fig. 2 indiciates that the loading is most sensitive to the density immediately in front of the antenna. Figure 2 also shows the effect of varying the outer gap on the loading. The main effect of varying the outer gap is to vary the density in the immediate vicinity of the antenna. In diverted discharges with similar outer gap and density, the loading is about 20% lower.

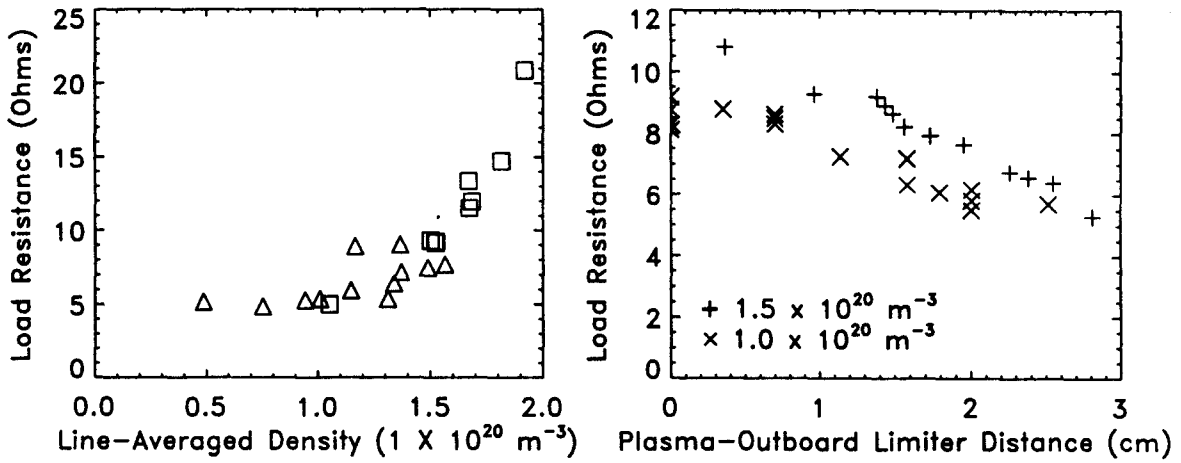

Figure 2 - Antenna loading vs. density and outer gap

Heating Significant heating is observed when high power is applied. Figure 3 shows data from a discharge where 1.65 MW of rf power is applied to an inner wall limited plasma with $\kappa = 1.5$ and a line-averaged density of 1.8×10^{20} m^{-3}. The stored energy as determined by magnetic equilibrium reconstruction (EFIT) increases by more than 30 kJ, the electron temperature at the sawtooth peak measured by ECE increases by 1.4 keV (the average increase is about 0.6 keV), and the ion temperature measured from the neutron rate increases by 0.6 keV. The diamagnetic stored energy shows a similar increase to the EFIT value and the instantaneous change in slope of the diamagnetic signal at rf turn on and turn off is consistent with absorption of 80-100% of the rf power. The ion temperature measured by Doppler broadening of Argon lines agrees well with the neutron rate measurement and the Doppler measurements show that the ion temperature increases across most of the profile. The ECE data shows an increase of the sawtooth period from 5 to 15 ms and the Ohmic heating power decreases from 1.1 to 0.8 MW. While fewer experiments have been done in diverted discharges thus far, the same rf power levels have been applied with similar heating observed.

Impurity Generation The increases in radiated power and Molybdenum radiation are significantly reduced using the two-strap antenna with dipole phasing, as has been observed on many experiments. It is important to note that this improvement is also observed in the all-Molyndenum environment of Alcator C-Mod. The Molybdenum radiation is observed to increase linearly with rf power, but with the dipole antenna the magnitude is down by as much a factor of ten at 500 kW. The total radiated power, as measured by a bolometer array, which was as much as 100% of the rf power for the single-strap antenna in diverted discharges, now is about 50-60% for rf-heated limiter discharges, with a similar 50% radiated in Ohmic limiter plasmas.

Confinement Analysis of the heating data from a large number of limiter discharges varying rf power, density, and plasma current shows good agreement with ITER89-P L-Mode scaling.[2]At low current, the rf power can be three times the Ohmic power while at high current, it is about equal to the Ohmic value. The ASDEX-U H-mode scaling indicates that the threshold power for Alcator C-Mod at 5.3 T and $\overline{n}_e = 1 \times 10^{20}$ m^{-3} is about 1.5 MW. H-modes have been previously observed in Ohmic plasmas at fields up to 5.3 T.[6]

Brief periods with H-mode signatures have been observed during ICRF heating, of inner wall limited discharges which were nearly but not quite diverted. ELMing H-modes of 40 ms duration (about twice τ_e) and ELM-free periods of 12 ms. have been observed. Figure 4 shows an example of a brief ICRF-produced ELM-free H-mode period. The ICRF H-modes are difficult to maintain because the 30% (ELMing) to 45% (ELM-free) decrease in loading causes a reduction

or an interruption of the rf power. The H-modes are identified by the characteristic drop in H_α at the edge and a concommitant density increase. During the ELM-free period, the diamagnetic stored energy continues to rise despite the sudden reduction in rf power from 1.4 to 0.8 MW, implying at least a transient increase in energy confinement. All of these effects can be seen in Fig. 4, which also shows that at the lowest loading, peak rf voltages of up to 39 kV are supported by the antenna and matching systems.

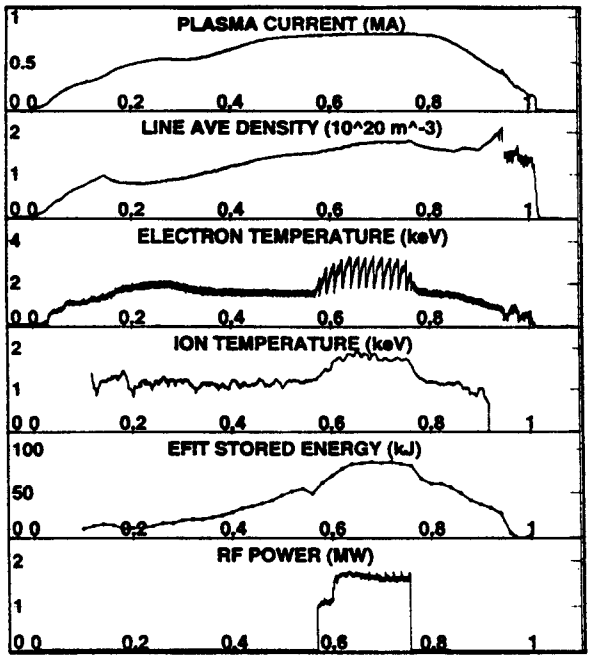

Figure 3 - Parameters with ICRF heating

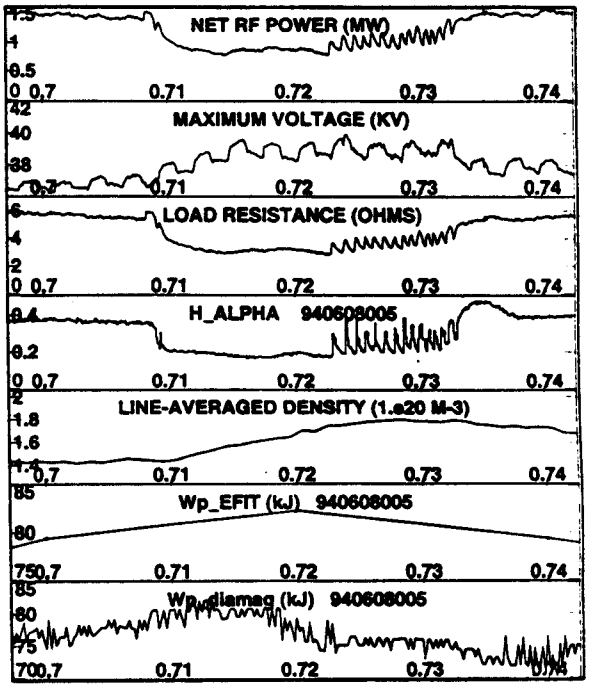

Figure 4 - Transient ELM-free ICRF H-mode

Conclusions The initial results of ICRF heating experiments using a two-strap antenna with dipole phasing are very encouraging. Effective plasma heating and control of rf-related impurity generation have been demonstrated in a tokamak with molybdenum plasma facing components. The energy confinement shows L-mode scaling and brief periods of H-mode behavior have also been observed. The first of two two-strap antennas has been operated up to 1.8 MW and experiments with two such antennas and 4 MW of available rf power will begin in the near future.

Acknowledgements It is a pleasure to acknowledge the numerous contributions of the Alcator engineering and technical staff. We are particularly grateful to M. Fridberg and W. Beck for engineering of the rf transmitters and antenna systems respectively. This work was supported by USDOE Contract No. DE-AC02-78ET51013.

References

[1] I. H. Hutchinson et al., *Phys Plasma* 1, 1511 (1994).
[2] I. H. Hutchinson et al., Contr. Fusion Plasma Physics (21st European Conference, Montpellier, 1994), invited paper.
[3] S. N. Golovato et al., in *Proceedings of the 9th Topical Conference on Radio-Frequency Power in Plasmas*, Charleston, SC (AIP, New York, 1991), p. 185.
[4] Y. Takase et al., *Fusion Eng. and Design*, 1994 (to be published).
[5] Y. Takase et al., in *Proceedings of the 9th Topical Conference on Radio-Frequency Power in Plasmas*, Charleston, SC (AIP, New York, 1991), p. 189.
[6] J. A. Snipes et al., *Nucl. Fusion*, 1994 (to be published); J. A. Snipes et al., Contr. Fusion Plasma Physics (21st European Conference, Montpellier, 1994), post-deadline paper.

ICRF and Ohmic H-modes in Alcator C-Mod

J. A. Snipes, R. S. Granetz, M. Greenwald, I.H. Hutchinson,
D. Garnier, S. N. Golovato, J. Irby, B. LaBombard,
T. Luke, E. S. Marmar, M. Porkolab,
Y. Takase, J. L. Terry

MIT Plasma Fusion Center
Cambridge, MA, USA

Introduction Transitions to high particle and energy confinement regimes have been achieved in Alcator C-Mod under a variety of operating conditions including lower single null diverted with ohmic heating alone of about 1 MW, with ICRH up to 1.5 MW, and inner wall limited with ICRH. ELM-free ohmic H-modes were obtained by ramping down the toroidal field to about 3 T. ELMy ohmic H-modes have been achieved even with constant toroidal field up to 5.25 T and densities with $\bar{n}_e \leq 1.4 \times 10^{20}$ m^{-3}. Both ELMy and ELM-free ICRF H-modes have been obtained with constant toroidal field up to 5.37 T and densities with $\bar{n}_e \leq 1.8 \times 10^{20}$ m^{-3}. In ELM-free H-modes, particle confinement improves by 50 - 100% while energy confinement improves by $\geq$ 50%, typically. The H-modes are short-lived with ELM-free durations of $\leq$ 50 msec before the rapidly increasing density returns the plasma to L-mode. In both ohmic and ICRF ELM-free cases, the threshold input power required to achieve H-mode appears to fit the scaling found on other tokamaks, $P/S\ (MW/m^2) = 4.4 \times 10^{-3}\ \bar{n}_e B_T\ (10^{19}\ m^{-3}\ T)$ [1], but the threshold power in ELMy cases at higher toroidal field can be as little as half of the value predicted by the scaling law. Note that the ICRF antenna Faraday shields and protection tiles are coated with either titanium carbide or boron carbide while the inner wall, outboard limiter, and divertor target are all molybdenum components, which withstand power densities up to at least 0.33 MW/m^2 with no degradation in plasma performance ($1.2 < Z_{eff} < 1.7$). No special wall coating techniques were necessary to achieve most of these H-modes, though the lowest power threshold ELMy H-modes at higher toroidal field were obtained after injecting lithium pellets into the plasma, which may have helped condition the plasma facing components to reduce recycling and impurity influxes.

Ohmic H-Modes The first ELM-free ohmic H-modes in C-Mod [2] were achieved by ramping the toroidal field down at constant plasma current of 0.65 MA so that the power threshold for H-mode was exceeded at $B_T \approx 3$ T, $P_{OH} \approx 1$ MW, and $\bar{n}_e \approx 1.0 \times 10^{20}$ m^{-3}. The density rose rapidly for up to 50 msec until the plasma either returned to L-mode confinement or disrupted at $q_\psi = 2$ (Fig. 1). The confinement analysis is complicated by the short duration of these H-modes and the rapidly changing density and plasma stored energy, but estimates of the confinement time, not including dW/dt corrections, are between 40 msec $< \tau_e <$ 60 msec, which is in the range of the ITER H-mode scaling [3]. Typical H-mode

enhancement factors are approximately 2. Estimates of the particle confinement time from absolutely calibrated H_α and interferometer measurements indicate an increase of 100%, typically.

ELMy ohmic H-modes have also occurred early in the rampdown of the toroidal field at the end of the discharge as well as during the flattop with toroidal fields from 4 T < B_T < 5.25 T. These H-modes lasted from 40 - 300 msec, showed characteristic rapid (5-6 kHz) ELM oscillations on the H_α emission near the X point, and only modest (20%) increases in the density and stored energy. The H-modes at higher toroidal field (B_T > 5 T) occurred after the injection of lithium pellets. The first such high field H-mode occurred during the density decay immediately after a single Li pellet, while others occurred 10 - 14 discharges after a series of discharges in which 12 Li pellets had been injected, each pellet being equivalent to about a monolayer of Li on the plasma facing components. It is possible through erosion and redeposition of the lithium, that the Li wall coatings from the previous discharges continued to reduce the D recycling and the influx of impurities from the walls, much like the lithium wall conditioning observed during supershots in TFTR [4]. Further experiments are planned to test this hypothesis.

ICRF H-Modes Fixed frequency (80 MHz) Ion Cyclotron Resonant Frequency (ICRF) waves have been coupled to the plasma with up to 1.8 MW of injected power [5]. Short (10 - 15 msec duration) ELM-free H-modes have been achieved with only 1.5 MW of ICRH and longer (~50 msec duration) ELMy H-modes were obtained with 1 MW < P_{ICRH} < 1.5 MW at constant $B_T \approx 5.3$ T and densities in the range of $1.2 < \bar{n}_e < 1.8 \times 10^{20}$ m^{-3}. The duration of these H-modes is often limited by the loss of coupling of the RF power due to reduced loading during the H-mode. Figure 2 shows a discharge with two ICRF H-modes that both start with a short ELM-free phase followed by a short ELMy phase. Both H-modes begin during the RF heating at the collapse of a large sawtooth, but the second H-mode continues for about 15 msec even after the RF is switched off. The particle confinement improves by at least a factor of 2, but the energy confinement is difficult to assess because of the short duration of the H-mode.

Figure 3 shows an example of a discharge with several ELMy ICRF H-modes. Three ELMy periods lasting 20 - 30 msec each are seen with short transitions back to L-mode. The RF coupling to the plasma is reduced during the H-mode, reducing the injected power, which then makes it more difficult to maintain the H-mode. Then, as the plasma returns to L-mode, the RF coupling improves and the power increases, causing another transition back to H-mode. A frequency feedback system should help maintain good RF coupling with the rapid changes in density during H-modes. The stored energy remains constant even when the RF power drops by 30%, indicating a somewhat improved energy confinement. The particle confinement improves by nearly 100% during the ELMy H-mode periods. At the bottom of Fig. 3 are shown the ELM oscillations on the H_α emission from the divertor and on an inner wall poloidal field pick-up coil during the decay of the RF power. The ELMs stop briefly while $(dP/dt)_{ICRH}$ is large, then continue for about 10 msec after the RF power turns off.

Power Threshold With the addition of ICRH, the H-mode power threshold scaling has been extended to power densities of 0.33 MW/m^2, about a factor of two over previous C-Mod results [2], and with the addition of a second ICRF dipole antenna later this year, the scaling should be extended by another factor of two and be in the range of values expected for ITER. Figure 4 compares the H-mode threshold power scaling with previously published data from other tokamaks [1,6]. Although the number of ELM-free H-modes with ICRF is quite limited, the results agree with the previous scaling for the threshold power. The ohmic and ICRF ELMy H-modes, however, often tend to have a lower power threshold by as much as 30% without wall conditioning, other than standard electron cyclotron discharge cleaning before each run. In the series of discharges with Li pellet injection before ohmic ELMy H-modes, the threshold power was found to be significantly reduced by as much as a factor of two below the expected scaling. As has been found with other tokamaks, wall conditioning can play a significant role in lowering the H-mode threshold power. Nonetheless, with molybdenum plasma facing components and no special wall conditioning, H-modes have been readily achieved even up to rather high power densities with no significant impurity influx problems.

Conclusion The high electron density, high toroidal field, and high power density of Alcator C-Mod extend the H-mode regime of the world's divertor tokamaks to significantly higher values that now approach those expected for ITER. Although these are initial results, they indicate that the previous scaling of the H-mode threshold power with $\bar{n}_e B_T$ can be extended up to ITER values with approximately the same coefficient of 0.040 $(MW/m^2)/(10^{20} m^{-3}\ T)$ for ELM-free H-modes, but may need to be significantly reduced by 30 - 50% for ELMy H-modes depending critically on the material and condition of the plasma facing components. The initial C-Mod data have been included in the ITER H-mode database for scaling studies and this and future higher power ICRF data will greatly extend the range of the database.

References

[1] Ryter, F., Gruber, O., Büchl, K., Field, A.R., Fuchs, C., et al., in Controlled Fusion and Plasma Physics (Proc. 20th Eur. Conf. Lisboa, 1993), Vol. 17C, Part I, European Physical Society (1993) I-23.

[2] Snipes, J.A., Granetz, R.S., Greenwald, M., Hutchinson, I.H., et al., to be published in Nuclear Fusion.

[3] Ryter, F., Gruber, O., Kardaun, O.J.W.F., et al, Nucl. Fus., **33** (1993) 979.

[4] Snipes, J.A., Marmar, E.S., Terry, J.L., et al., J. Nucl. Mat. **196-198** (1992) 686.

[5] Golovato, S., Takase, Y., et al., this conference.

[6] Osborne, T.H., Brooks, N.H., Burrell, K.H., Carlstrom, T.N., Groebner, R.J., et al., Nucl. Fus., **30** (1990) 2023.

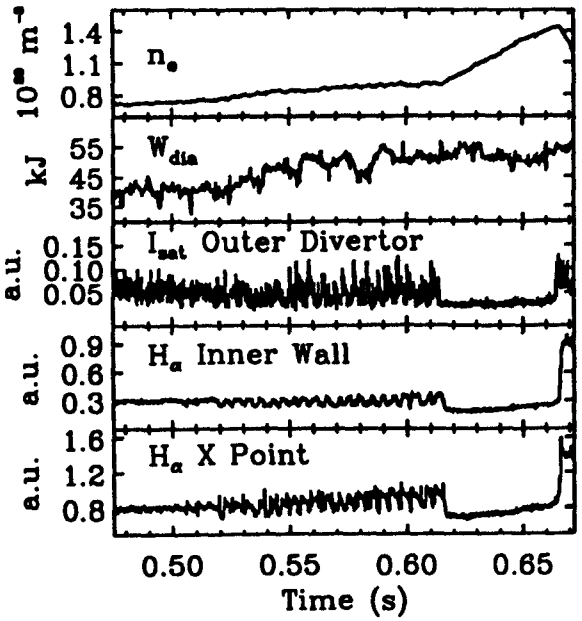

Fig 1. Dithering ohmic H-mode from 0.52 sec to 0.615 sec, then ELM-free until 0.665 sec showing the line averaged density, stored energy, divertor ion saturation current, inner wall and X point H_α.

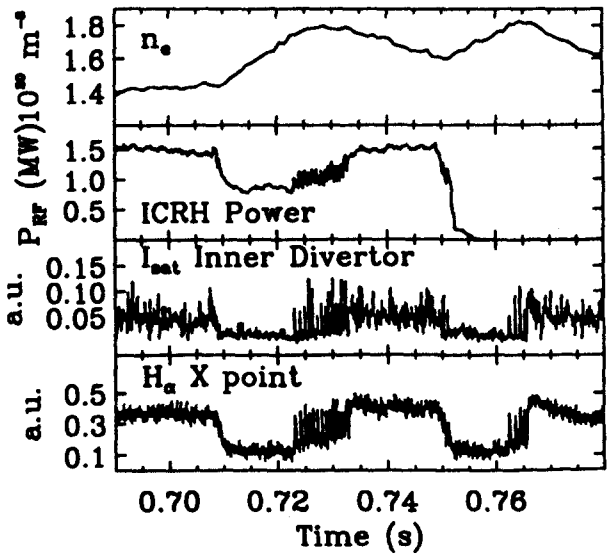

Fig. 2. Two ELM-free then ELMy RF H-modes from 0.71 to 0.735 sec and from 0.75 to 0.767 sec showing the line averaged density, ICRH power, divertor ion saturation current, and X point H_α.

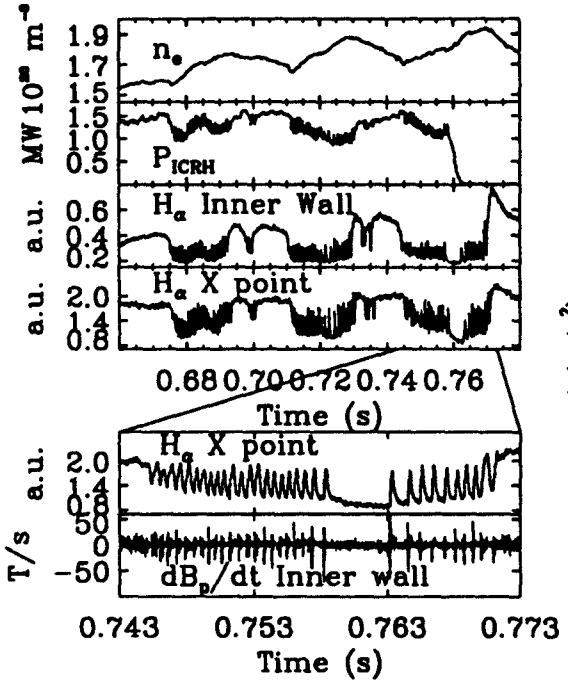

Fig. 3. Series of ELMy RF H-modes from 0.675 sec to 0.772 sec showing the line averaged density, ICRH power, inner wall and X point H_α. Zoomed time traces showing ELMs on the X point H_α and an inner wall poloidal field pick-up coil signal.

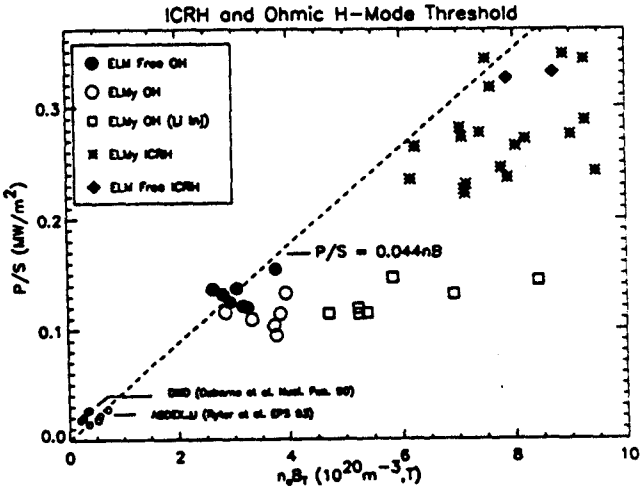

Fig. 4. H-mode threshold power density versus product of the line averaged density and the toroidal field for ohmic and ICRH, ELMy and ELM-free discharges, with and without lithium pellets compared to published data from ASDEX-Upgrade and DIII-D.